Mapping of poynting flux of dispersive Alfvén waves

N. Singh

Department of Electrical and Computer Engineering, University of Alabama, Huntsville, Al 35899, USA

Abstract. We theoretically determine the group velocity vector of Alfvén waves having narrow structures transverse to an ambient magnetic field. The theory is used to determine the width of such wave structures as they propagate downward from high altitudes where satellite observations are normally made. We predict that for very narrow structures in the regime of inertial and kinetic Alfven waves the Poynting flux maps with altitude r as S (r)~B(r)$^{1/2}$, in contrast to the commonly assumed mapping relation S (r)~B(r). We check our predictions using conjunction between FAST and Polar and between Polar and Geotail.

Index Terms. Alfvén waves, poynting flux, resonance cones.

---

1. Introduction

There are now several satellite measurements of Alfvén waves and their power densities, the Poynting flux **S** (Wygant et al., 2000, 2002; Domback et al., 2005; Angelopoulos et al., 2002; Chaston et al., 1999). While mapping the measured S along the geomagnetic field lines, it is common to assume that S(r)~B(r), where B is the magnetic flux density and r is the geocentric distance. This assumption holds good only for non-dispersive Alfvén waves with perpendicular wave number $k_\perp \cong 0$ having scales transverse to the geomagnetic fields of the order of the geophysical scale lengths. The measured waves are often narrow structures transverse to **B,** implying not only relatively large values of $k_\perp$, but also a broad spectrum of $k_\perp$. Such waves are dispersive and the propagation of energy depends on both parallel and perpendicular components of the group velocity vector $\mathbf{V_g}$ (Stasiewicz et al., 1997; Singh, 1999). The mapping using S(r)~B(r) tacitly assumes that $V_{g\perp}\sim 0$. The purpose of this paper is to theoretically explore the parametric behavior of $\mathbf{V_g}$ depending on the plasma parameters, such as the plasma density, and electron and ion temperatures as the geocentric altitude r varies covering the satellites such as FAST, Polar and Geotail. Fortunately, there are measurements of S during magnetic conjunctions between FAST and Polar (Domback et al., 2005) and also between Polar and Geotail (Angelopoulos et al., 2003) to check the theoretical predictions. We specifically show that for very narrow structures conforming to the dispersion relation of inertial and kinetic Alfvén waves, the mapping is according to S (r)~B(r)$^{1/2}$.

2. Group velocity for dispersive Alfven waves

A useful dispersion relation for Alfvén waves with non-zero $k_\perp$ is given by (Lysak and Lotko, 1996)

$$\omega = k_{||} V_A[(1+ (k_\perp \rho_a)^2)/(1+ (k_\perp \lambda_s)^2)]^{1/2}, \qquad (1)$$

---

where $k_{||}$ is the parallel component of wave vector **k,** V_A is the Alfven velocity, $\rho_a=\rho_i\times (0.75+T_e/T_i)^{1/2}$, ρ_i is the ion Larmor radius, T_e and T_i are the electron and ion temperatures, and the electron skin depth $\lambda_s = C/\omega_{pe}$ with C and ω_{pe} as the velocity of light and the electron plasma frequency, respectively. The parallel ($V_{g||}$) and perpendicular ($V_{g\perp}$) components of the group velocity vector $\mathbf{V_g}$, given by $V_{g||}=\partial\omega/\partial k_{||}$ and $V_{g\perp}=\partial\omega/\partial k_\perp$, are

$$V_{g||}= V_A[(1+ k_\perp^2 \rho_a^2)/(1+ k_\perp^2 \lambda_s^2)]^{1/2}, \qquad (2)$$

$$V_{g\perp}=V_A k_{||} k_\perp [(1+ k_\perp^2 \rho_a^2)/ (1+ k_\perp^2 \lambda_s^2)]^{-1/2} G(k_\perp), \qquad (3)$$

$$G(k_\perp)=\rho_a^2[1+ k_\perp^2 \lambda_s^2]^{-1}- \lambda_s^2[1+ k_\perp^2 \rho_a^2] [1+ k_\perp^2 \lambda_s^2)]^{-2}. \qquad (4)$$

For the angle θ made by $\mathbf{V_g}$ from $\mathbf{B_o}$, given by $\tan(\theta)=V_{g\perp}/V_{g||}$ and using $\tan(\theta)\sim\theta$ for small θ, we have

$$\theta\sim(\omega/\Omega_i)(m/M)^{1/2} k_\perp[(1+ k_\perp^2)/ (1+ k_\perp^2 \alpha^2)]^{1/2} \times[\alpha^2(1+ k_\perp^2 \alpha^2)^{-1}- (1+ k_\perp^2)^{-1}] \qquad (5)$$

Note that in writing (5) we have expressed $k_\perp$ in units of $k_s=1/\lambda_s$, that is, $k_\perp\lambda_s\rightarrow k_\perp$, and $\alpha=\rho_a/\lambda_s$. The parameter α is an important quantity; it determines the nature of the dispersion whether the wave is inertial (IA) or kinetic (KA) Alfvén wave (Singh, 1999). Physically α^2 is related to the plasma β; $\alpha^2=(\rho_a/\lambda_s)^2\sim(M/m)[(0.75T_i+T_e)/M](\omega_{pi}/C\Omega_i)^2\sim (V_{teff}/V_A)^2 \sim(M/m)\beta$, where β is the ratio of plasma kinetic to magnetic energy density. M and m are the ion and electron mass respectively. We find that when $\alpha^2= 1$ or $V_A\sim V_{eff}$, the effective electron thermal velocity, or equivalently β~m/M, θ~0. When $\alpha^2<<1$, θ is negative and it implies that the IA waves in this regime are backward wave in the direction

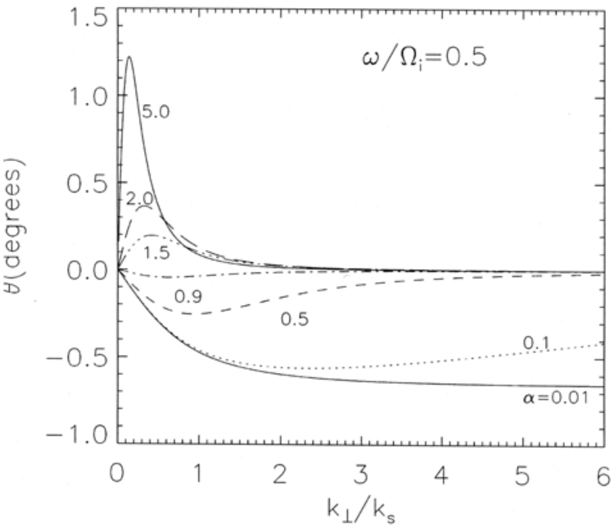

Fig. 1. Group velocity cone angle as a function of perpendicular wave number $k_\perp\lambda_s$ for several values of $\alpha=\rho_a k_s$.

transverse to $\mathbf{B_o}$. On the other hand when α^2>>1, the KA waves have θ>0. Fig. 1 shows a series of curves showing $\theta(k_\perp)$ for several values of α. As expected, there are two distinct families of curves for the KA and IA waves. KA waves have θ>0 while IA waves have θ<0. For the IA waves the curve for α=0.01 is like that in a cold plasma (Singh, 1999). As α increases, the warm plasma effects yield a maximum in $|\theta(k_\perp)|$. For α=1, $\theta(k_\perp)$=0, implying that inertial and warm plasma effects cancel each other. For α>1, KA waves have peaked $\theta(k_\perp)$. Both regimes of propagation show that there is a maximum angle depending on α. These maximum angles determine the maximum spreading of the wave power across $\mathbf{B_o}$ as a wave structure, narrow across $\mathbf{B_o}$, propagates along the magnetic field.

It is possible to determine the maximum group velocity angles in the IA and KA wave regimes. We find that in the IA regime, maximum value of θ is

$$\theta_{imax}\sim -(\omega/\Omega_i)(m/M)^{1/2}/(1+\alpha), \quad \alpha^2 <<1 \qquad (6)$$

and it occurs for $k_\perp \sim k_s/\alpha^{1/2} > k_s$. For all other values of $k_\perp$, $\theta < \theta_{imax}$. When $\alpha\rightarrow 0$, θ_{imax} becomes the same as the Alfvén wave resonance cone found from cold plasma description (Singh, 1999). For the IA waves propagating along $\theta_{imax,}$ the parallel phase velocity ($V_{p||}$) and the ratio of transverse components of electric (E) to magnetic (B) fields are

$$V_{p||}\sim V_A\alpha/(1+\alpha)\sim\alpha V_A,\ E/B\sim V_{p||}\sim\alpha V_A,\ \alpha^2<<1. \qquad (7)$$

Note that the ratio E/B is often used to test whether waves observed from satellites are Alfvén waves or not. For the KA waves, we obtain maximum angle

$$\theta_{kmax}\sim 2/(27)^{1/2}(\omega/\Omega_i)\,(m/M)^{1/2}\alpha\sim 2/(27)^{1/2}(\omega/\Omega_i)C_a/V_A, \quad \alpha^2>>1 \qquad (8)$$

and it occurs at $k_\perp\sim k_s/\ 2^{1/2}\alpha < k_s$. In (8) C_a is effective ion – acoustic speed defined by $C_a^{\ 2}=(0.75T_i+ T_e)/M$.

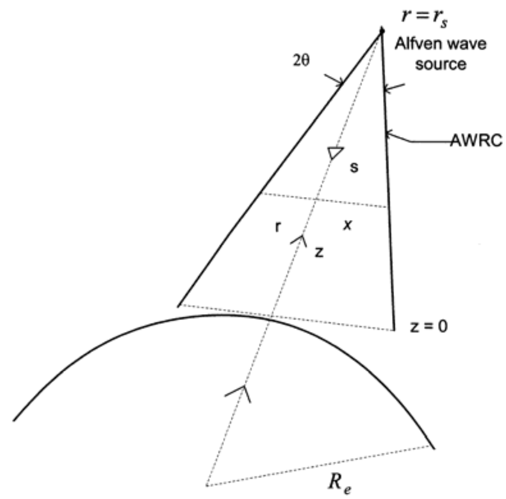

Fig. 2. Alfvén wave source is a line source at $r=r_s$, which generates waves propagating in a resonance cone structure of half cone angle θ. The line source extends in longitude.

3. Propagation within a cone from a narrow structure at large altitudes

A consequence of the group velocity vector making a small angle from $\mathbf{B_o}$ in both IA and KA wave regime is that the wave power diverges across $\mathbf{B_o}$ when launched from distant localized sources. This is schematically shown in Fig. 2.

The rate of divergence along the field line is

$$dX/ds\sim\tan(\theta)\sim\theta, \qquad (9)$$

where X is the half-width of the wave structure at distance s from the source at $r=r_s$. Using θ_{imax} for IA waves and θ_{kmax} for the KA waves, the above equation can be integrated from $r=r_s$ to any altitude r to yield the total width of the wave structure W(r). For the KA waves, this integration might require numerical methods depending upon the electron and ion temperature profiles $T_e(r)$ and $T_i(r)$. For the IA waves, the integration is straight forward if one assumes that the plasma is dominated by H^+ over the altitude range of interest, and the magnetic field is given by $B(r)\sim B_e(R_e/r)^3$:

$$W(r)=2X(r)= (1/2)(m/M_i\,)^{1/2}(\omega/\Omega_{ie})\ [\ (r_s\,/R_e\,)^4-(r\,/R_e\,)^4\,]R_e, \qquad (10)$$

where B_e and Ω_{ie} are the earth’s magnetic field and ion cyclotron frequency at $r=R_e$, respectively. It is interesting to note, that (10) approaches an asymptotic limit when the height z (Fig. 2) is sufficiently small so that $r(s)\sim R_e$ and $(r(s)/r_s)^4 << 1$, giving the width

$$W\sim (1/2)(m/M_i)^{1/2}(\omega/\Omega_{is})\ r_s. \qquad (11)$$

This is a constant width with variation in the altitude depending on electron to ion mass ratio, wave frequency and the source location r_s and it gives the absolute minimum latitudinal width; this is the transverse size of the IA wave when exited by an ideal line source at $r=r_s$ with the latitudinal source width $x_s \sim 0$, like for a line source extending in longitude. If we assume a H^+ plasma we find that $X(s)=5.8\times10^{-3} (\omega/\Omega_{is}) r_s$, and the transverse width (W) of an IA wave structure is

$$W/R_e = 2X/R_e = 1.2 \times10^{-2} (\omega/\Omega_{he}) (r_s/R_e)^4, \qquad (12)$$

where Ω_{he} is the H^+ ion cyclotron frequency at $r=R_e$. If we assume $r_s \sim 18R_e$ and $\omega \sim 6.28$ rad/s (1 Hz), we find that W~3 km at ionospheric altitudes, comparable to the widths of narrow auroral arcs.

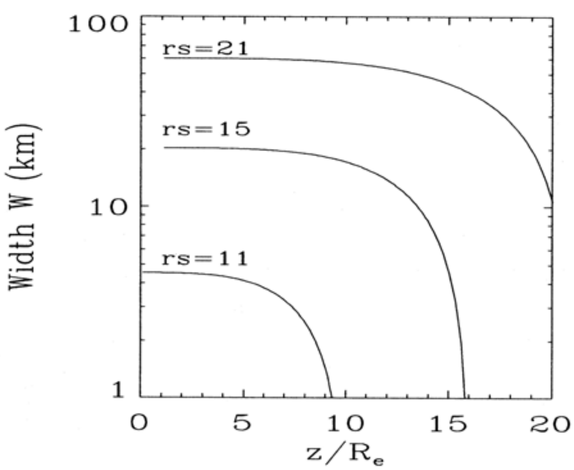

Fig. 3. W(z) as a function of altitude z for r_s =11, 15 and 21 R_e when f = 2 mHz. Note that W becomes asymptotically constant at lower altitudes in H^+ plasma.

Fig. 3 shows W(z) as a function of z from (10) for three source locations r_s/R_e = 11, 15 and 21 when frequency f= 2 mHz. Note that for sufficiently small z ($r \ll r_s$), the curves for W become flat giving a constant width of the wave structure as noticed earlier (see (12)). For the altitudes of observations of IAWs by Polar ($z \sim 3\text{-}4R_e$), the widths range over 4-60 km as the source location varies from r_s=11 to 21 R_e for f=2 mHz. The constancy of W with r at sufficiently large distance from the source seen for the IA waves also holds good for the KA waves. This is more so because the cone angle $\theta_{kmax} \sim B(r)^{-2}$ due to the factors Ω_i (~B) for the KA waves and V_A (~B) being in the denominator of eqn. (8) for θ_{kmax}.

4. Application to satellite observations

The constancy of W has the following implications for the scaling of the Poynting flux (S). Wygant et al. suggest that S=1-2 ergs cm^{-2} s^{-1} (1-2 $mWatt/m^2$) at the altitude of measurements of IAWs by Polar and when mapped to ionospheric altitudes along converging magnetic field lines S~100 ergs cm^{-2} s^{-1} (0.1 $Watt/m^{-2}$). In contrast, in view of the constant width of the narrow Alfvén wave structures with the decreasing altitude to the ionospheric heights the power flux must not increase directly with increasing B. The increase might result only partially due to the convergence of B in longitude giving $S \sim B^{1/2}$. Thus, in case of the Polar observation the power density at the ionospheric altitudes might just be 10 ergs cm^{-2} s^{-1}, an order of magnitude smaller than suggested by (Wygant et al. 2000). We support this claim from two studies based on magnetic conjunction between Polar and FAST and Geotail and Polar.

Polar-FAST conjunction

We find that simultaneously measured maximum fluxes from Polar and FAST during the condition of magnetic conjunction along night-side auroral field lines support the scaling $S \sim B^{1/2}$. The data is reported in Fig. 3 of (Dombeck et al. 2005). As normally done, Dombeck et al (2005) map the values S as measured by Polar and Fast to 100 km ($1.06R_e$) altitude in the ionosphere. At the time of the conjunction, geocentric distance of FAST and Polar are r_f= $1.549R_e$ and $r_p=7.1R_e$; the subscripts 'p' and 'f' refer to Polar and FAST, respectively. Thus the normal mapping amplifies measured S by a factor 300 for Polar and 3 for FAST. The mapped maximum fluxes at 5mHz from FAST and Polar are S_f=1 and S_p=10 mW/m^2, giving actual wave energy fluxes at the satellites $S_f(r=r_f)$=0.33 and $S_p(r=r_p)$=0.033 mW/m^2. Thus we find that actual fluxes at the satellites have a ratio S_f/S_p= $(r_p/r_f)^{3/2} \cong$ 10, supporting our suggestion that $S \sim B^{1/2}$ for narrow structure Alfvén waves.

Geotail-Polar conjunction

Angelopoulos et al. (2002) compared the Alfven wave Poynting fluxes measured by Polar and Geotail during a magnetic conjunction. They report a peak flux S_g =0.23 mW/m^2 during a wave event of extremely narrow Alfven wave structure detected with full resolution from Geotail at $r \sim 18R_e$. The corresponding flux at Polar was S_p=1.25 mW/m^2 at $r=5R_e$. The unperturbed magnetic fields at the satellites are given as B_p~280 nT and B_g~18 nT. Using the usual scaling S~B, the measured flux at Geotail translates to 0.23× (280/18)~ 3.6 mW/m^2 at Polar. Thus there is a loss of 2.35 mW/m^2 and it was attributed to the energization of electrons and ions in the intervening distance between the satellites. However, the flux balance was not demonstrated by including particle energy fluxes. In view of the latitudinal constancy of the widths of KA waves, the flux expected at Polar should be only 0.23× $(280/18)^{1/2}$ ~ 1 mW/m^2. In view of all the uncertainties in averaging of fluxes at the two satellites, this estimate seems to be in good agreement with the flux measured at Polar.

5. Conclusion

Our primary conclusion is that while mapping Poynting flux of dispersive Alfven waves measured by high-altitude satellites to low altitudes, its divergence due to non-zero perpendicular group velocity must be *properly* accounted. It turns out that narrow Alfven wave structures attain a constant width in latitude and therefore the convergence in S due to increasing B with decreasing r is given by $S \sim B^{1/2}$ and not commonly used mapping S~B.

Acknowledgement. This work was supported by NASA grants NAG513489.

References

V. Angelopoulos, J.A. Chapman, F.S. Mozer, J.D. Scudder, C.T. Russell, K. Tsuruda, T. Mukai, T.J. Hughes and K. Yumoto, "Plasma sheet electromagnetic power generation and its dissipation along auroral field lines", *J. Geophys. Res*., vol. 107, doi:10.1029/2001JA900136, p. 1181, 2002.

P. M. Bellan, "New model for ULF Pc5 Pulsations: Alfvén Cones", *Geophys. Res. Lett*., vol. 23, p. 1717, 1996.

C. C. Chaston, et al., "Fast Observations of inertial Alfvén Waves in the dayside aurora", *Geophys. Res. Lett*., vol. 26, p. 647, 1999.

J. Dombeck et al., "Alfvén waves and Poynting flux observed simultaneously by Polar and FAST in the plasma sheet boundary layer", *J. Geophys. Res.*, in press, 2005.

R. L. Lysak and W. Lotko, "On the dispersion relation for shear Alfvén Waves", *J. Geophys. Res.* vol. 101, p. 5085, 1996.

N. Singh, "Field patterns of Alfvén wave resonance cones", *J. Geophys. Res.* vol.104, pp. 6999, 1999.

K. Stasiewicz et al., "Cavity resonance and Alfvén resonance cones", *J. Geophys. Res*., vol. 102, p. 2565, 1997.

J. R. Wygant, A. Keiling, C. A. Cattell, R. L. Lysak, M. Temerin, F. S. Mozer, C.A. Kletzing, J. D. Scudder, V. Streltsov, W. Lotko and C.T. Russell, "Evidence for kinetic Alfvén waves and parallel electron energization at 4–6 R_E altitudes in the plasma sheet boundary layer", *J. Geophys. Res*., vol. 107, doi:10.1029/2001JA900113, p. 1201, 2002.

J. R. Wygant, A. Keiling, M. Johnson, C. A. Cattell, R. Lysak, M. Temerin, F. S. Mozer, C. A. Kletzing, J. D. Scudder, W. Peterson, C. T. Russell, G. Parks, M. Brittnacher, G. Germany and J. Spann, "Polar spacecraft based comparisons of intense electric fields and Poynting flux near and within the plasma sheet-sheet boundary to UVI images: An energy source for the aurora", *J. Geophys. Res*., vol. 105, p. 18675, 2000.